

Light-Mediated C–C σ -Bond Driven Crystallization of a Phenalenyl Radical Dimer

Puhong Liao,[†] Mikhail E. Itkis,[†] Richard T. Oakley,[‡] Fook S. Tham,[†] and Robert C. Haddon^{*†}

Contribution from the Departments of Chemistry and Chemical & Environmental Engineering, University of California, Riverside, California 92521-0403, and Department of Chemistry, University of Waterloo, Waterloo, Ontario N2L 3G1, Canada

Received June 24, 2004; E-mail: haddon@ucr.edu

Abstract: Polymorphism—the phenomenon that a given compound forms more than one crystalline arrangement of the molecules in the solid state—plays a crucial role in understanding organic conductors, superconductors, and magnets. We have found that solutions of a new phenalenyl radical can give rise to two (nonpolymorphic) crystalline forms depending on whether the crystallization is allowed to proceed in the presence or absence of light. In both cases the crystals take the form of black shining blades and are indistinguishable by optical microscopy. We have fully characterized these crystalline forms, and we show that they differ by the presence or absence of a C–C σ -bond between the unpaired electrons of the parent radical. These molecular forms crystallize from the same solvent to give rise to a σ -dimerized insulator and a monomeric radical semiconductor as dictated by the presence or absence of light.

Introduction

Polymorphism—the phenomenon that a given compound forms more than one crystalline arrangement of the molecules in the solid state—often plays a crucial role in the electronic structure of organic conductors, superconductors, and magnets.^{1–3} Steric factors usually determine the persistence of neutral carbon-centered radicals,⁴ which may crystallize in different forms depending on the choice of solvent.^{5,6} In this paper we report light-mediated carbon–carbon σ -bond driven dimerization of a new phenalenyl radical, together with full characterization of the solid-state radical and dimer, which consist of an organic semiconductor and an organic insulator.

For some time, we have attempted to prepare an intrinsic molecular metal, that is, a solid composed of a single molecular species that would function as a classical (mon)atomic metal and superconductor.⁷ Unless elemental metals are involved,⁸ this requires the crystallization of a neutral radical, and we have argued in favor of the phenalenyl system. The spirobiphenalenyls that we proposed avoid the problems associated with an exactly half-filled band and also circumvent the 1-dimensionality that is associated with many planar conjugated π -systems. However, the present strategy does not address the question of σ -dimer-

ization.⁹ Nevertheless, all of the compounds reported to date in this series have consisted of monomeric free radicals or π -dimers with paramagnetic and diamagnetic states that are observable in different temperature regimes, and the neutral alkyl-substituted spirobiphenalenyl radicals possess unique solid-state properties (Scheme 1).^{9–12}

The hexyl radical **5** (R = C₆H₁₃) shows the highest conductivity of any neutral organic molecular solid, despite the fact that all intermolecular contacts are outside the van der Waals spacing. Changing the alkyl group from hexyl (**5**) to butyl (**3**) (R = C₄H₉) or ethyl (**1**) (R = C₂H₅) leads to crystal structures that contain π -dimers, which, in the case of **3**, gives a solid that exhibits bistability in three physical channels: electrical, optical, and magnetic.^{13,14} X-ray and magnetic susceptibility measurements show that these compounds usually exist as isolated free radicals with one spin per molecule (at least over some temperature range). Although we did not employ bulky substituents at the active positions of the phenalenyl nucleus to suppress intermolecular carbon–carbon bond formation, no σ -dimerization has been observed. Carbon-based free radicals usually require steric hindrance to suppress σ -dimerization in the solid state,^{4,15} and we are not aware of any other system where resonance stabilization has been sufficient to allow the

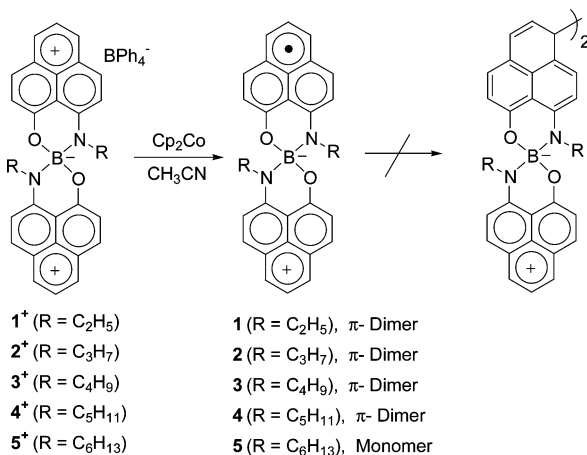
[†] University of California.

[‡] University of Waterloo.

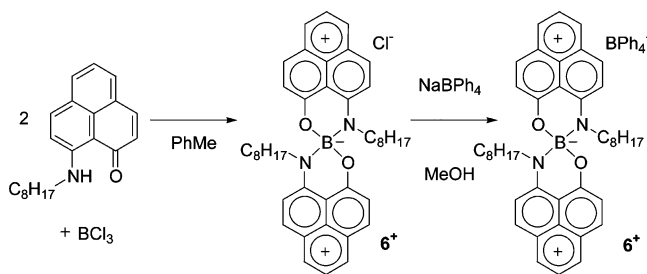
- (1) Bernstein, J.; Davey, R. J.; Henck, J. *Angew. Chem., Int. Ed.* **1999**, *38*, 3440–3461.
- (2) Bernstein, J. *Polymorphism in Molecular Crystals*; Clarendon Press: Oxford, 2002.
- (3) Miller, J. S. *Adv. Mater.* **1998**, *10*, 1553–1557.
- (4) Griller, D.; Ingold, K. U. *Acc. Chem. Res.* **1976**, *9*, 13–19.
- (5) Kahr, B.; Engen, D. V.; Mislow, K. *J. Am. Chem. Soc.* **1986**, *108*, 8305–8307.
- (6) Kahr, B.; Engen, D. V.; Gopalan, P. *Chem. Mater.* **1993**, *5*, 729–732.
- (7) Haddon, R. C. *Nature* **1975**, *256*, 394–396.
- (8) Tanaka, H.; Okano, Y.; Kobayashi, H.; Suzuki, W.; Kobayashi, A. *Science* **2001**, *291*, 285–287.

- (9) Chi, X.; Itkis, M. E.; Patrick, B. O.; Barclay, T. M.; Reed, R. W.; Oakley, R. T.; Cordes, A. W.; Haddon, R. C. *J. Am. Chem. Soc.* **1999**, *121*, 10395–10402.
- (10) Chi, X.; Itkis, M. E.; Kirschbaum, K.; Pinkerton, A. A.; Oakley, R. T.; Cordes, A. W.; Haddon, R. C. *J. Am. Chem. Soc.* **2001**, *123*, 4041–4048.
- (11) Chi, X.; Itkis, M. E.; Tham, F. S.; Oakley, R. T.; Cordes, A. W.; Haddon, R. C. *Int. J. Quantum Chem.* **2003**, *95*, 853–865.
- (12) Pal, S. K.; Itkis, M. E.; Reed, R. W.; Oakley, R. T.; Cordes, A. W.; Tham, F. S.; Siegrist, T.; Haddon, R. C. *J. Am. Chem. Soc.* **2004**, *126*, 1478–1484.
- (13) Itkis, M. E.; Chi, X.; Cordes, A. W.; Haddon, R. C. *Science* **2002**, *296*, 1443–1445.
- (14) Miller, J. S. *Angew. Chem., Int. Ed.* **2003**, *42*, 27–29.

Scheme 1



Scheme 2



realization of carbon-based free radical solids. The alkyl chains on the exocyclic nitrogens of **1–5** clearly affect the packing of the radicals in the crystals, but are not in a position to sterically inhibit reactions of the phenalenyl rings; nevertheless, we find that one of the crystalline forms of **6** (Scheme 1, R = C₈H₁₇) exists as a σ -dimer and that the occurrence domain¹ is dictated by the presence or absence of light.

Results and Discussion

Preparation, Solution Properties, and Crystallization of Radical 6a and σ -Dimer 6b Polymorphs. The synthesis of the radical precursor 6^+ ,BPh₄[−] followed the same procedure that was used for other salts (**1**⁺, **2**⁺, **3**⁺, **4**⁺, and **5**⁺) (Scheme 2). The salt 6^+ ,BPh₄[−] gave an air-stable but highly light sensitive yellow solid that could be purified by recrystallization from acetonitrile to give yellow crystals suitable for radical preparation and crystal growth.

The electrochemistry of the salt 6^+ ,BPh₄[−] is presented in Figure 1, and it may be seen that the compound shows a well-behaved double reduction; the disproportionation potential of $\Delta E^{2-1} = E_2^{1/2} - E_1^{1/2} = -0.36$ V is similar to that of other members of this series.

We used cobaltocene as reductant because the oxidation potential ($E^{1/2} = -0.91$ V) falls between the $E_1^{1/2}$ and $E_2^{1/2}$ reduction potentials of 6^+ ,BPh₄[−] (Scheme 3). Crystals of **6** were prepared by mixing solutions of 6^+ ,BPh₄[−] and cobaltocene in dry, degassed acetonitrile in a drybox. On overnight standing, black shining blades of **6a** and **6b** crystallized; the crystalline polymorphs cannot be distinguished by the eye, but can be identified by near-IR transmittance spectroscopy of single crystals. In the beginning, we usually obtained mixed phases.

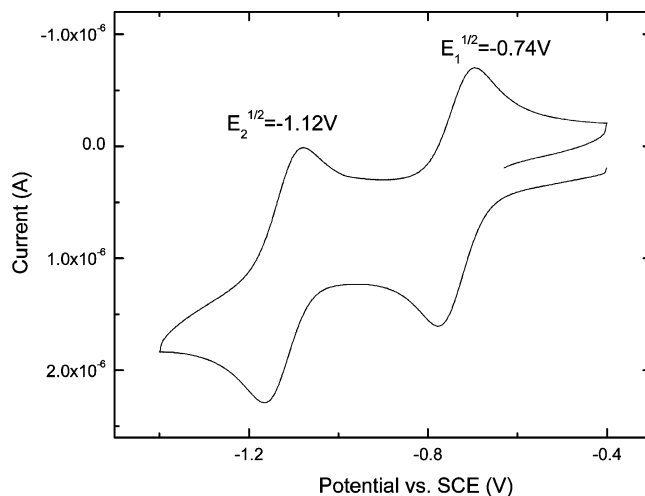
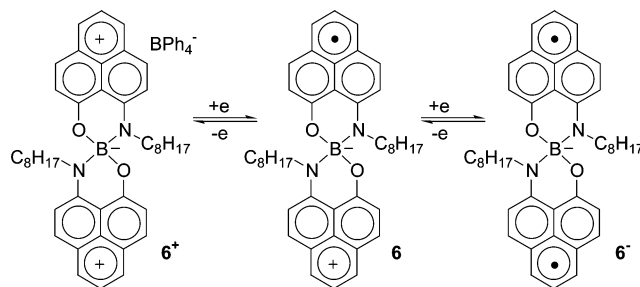
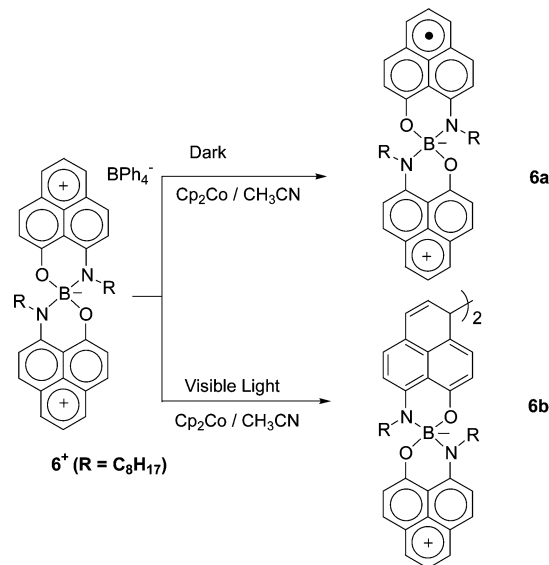


Figure 1. Cyclic voltammety of 6^+ ,BPh₄[−] in acetonitrile, referenced to SCE via internal ferrocene (not shown).

Scheme 3



Scheme 4



After investigating many variables that might be involved in the occurrence domain of the crystallization, we were able to identify light as the critical parameter. To generate the radical **6a**, rigorous exclusion of light was necessary (including the preparation of the acetonitrile solution of 6^+ ,BPh₄[−]) (Scheme 4). Exposure of the crystallization solution to visible light gave rise to crystals of the σ -dimer **6b**. Rigorous purification of the salts, reductants, and solvents, control of the concentration of the salt, and complete exclusion of light in the case of radical **6a** are required for the crystallization of **6a** and **6b** with reproducible yields in the form of large high-quality crystals.

(15) Goto, K.; Kubo, T.; Yamamoto, K.; Nakasuji, K.; Sato, K.; Shiomi, D.; Takui, T.; Kubota, M.; Kobayashi, T.; Yakusi, K.; Ouyang, J. *J. Am. Chem. Soc.* **1999**, *121*, 1619–1620.

Table 1. Crystal Data for 6^+ , BPh_4^- , **6a**, and **6b**

	6^+ , $\text{BPh}_4^- \cdot 2\text{CH}_3\text{CN}$	6a	6b
empirical formula	$\text{C}_{70}\text{H}_{74}\text{B}_2\text{N}_4\text{O}_2$	$\text{C}_{42}\text{H}_{48}\text{BN}_2\text{O}_2$	$\text{C}_{84}\text{H}_{96}\text{B}_2\text{N}_4\text{O}_4$
fw	1024.95	623.63	1247.27
cryst syst	triclinic	monoclinic	triclinic
space group	$P\bar{1}$	$P2(1)/c$	$P\bar{1}$
Z	2	4	1
temperature (K)	218(2)	223(2)	223(2)
unit cell dimensions	$a = 14.457(3) \text{ \AA}$ $b = 14.650(3) \text{ \AA}$ $c = 16.026(3) \text{ \AA}$ $\alpha = 73.246(4)^\circ$ $\beta = 67.638(4)^\circ$ $\gamma = 69.852(4)^\circ$	$a = 17.323(3) \text{ \AA}$ $b = 20.281(5) \text{ \AA}$ $c = 9.7394(17) \text{ \AA}$ $\alpha = 90^\circ$ $\beta = 93.740(6)^\circ$ $\gamma = 90^\circ$	$a = 9.1350(15) \text{ \AA}$ $b = 12.826(2) \text{ \AA}$ $c = 15.925(3) \text{ \AA}$ $\alpha = 103.674(4)^\circ$ $\beta = 98.411(4)^\circ$ $\gamma = 103.936(4)^\circ$
volume (\AA^3)	2898.2(9) \AA^3	3414.4(12) \AA^3	1718.2(5) \AA^3
goodness-of-fit on F^2	1.027	1.027	1.109
$R(F)$ ($F^2 > 2\sigma$) (R1)	0.0531	0.0671	0.0506
$R(F)$, wR2(F^2)	0.0840, 0.1631	0.1166, 0.2084	0.0821, 0.1468

Both crystalline polymorphs occur as black blades with the following typical dimensions: length 10–11 mm, width 300–400 μm , thickness 5–7 μm (**6a**) and length 4–5 mm, width 200 μm , thickness 46 μm (**6b**). Note that **6a** is thinner than **6b**, although many crystallization conditions were investigated to grow thicker crystals of **6a**. We conclude that solutions of the radical can generate either of the crystalline forms.

When fresh crystals of **6a** are put in contact with dry, degassed acetonitrile, a green solution of the radical is produced. However, the σ -dimer crystals are not easily redissolved, and acetonitrile that has been in contact with σ -dimer crystals is EPR silent. Addition of dichloromethane to such mixtures gives rise to a green solution with a strong EPR signal. Thus, it seems likely that the formation of the σ -dimer in acetonitrile solutions is kinetically slow, but once it is formed, crystallization is rapid. Both **6a** and **6b** readily dissolve in 1,2-dichlorobenzene to give solutions of the radical, as determined by cyclic voltammetric and EPR spectroscopic studies of the solutions.

We speculate that photoexcitations of the radicals in solution are responsible for the formation of the σ -dimer **6b**, and may involve excited states in which the unpaired electron becomes localized on a single phenalenyl ring. The energy levels in the radicals are complex,^{13,16} and C_{60} is known to undergo σ -dimerization upon irradiation. We cannot explain why this behavior does not occur with other members of the series (1–5).

X-ray Crystal Structures of 6^+ , BPh_4^- , **6a, and **6b**.** The X-ray crystal structures of 6^+ , BPh_4^- , **6a**, and **6b** (cation, radical, and σ -dimer, respectively) and the crystal data are summarized in Table 1. The distinctive features of the phenalenyl packing are weak π -dimers with a separation between phenalenyl rings of about 3.56 \AA (cation), π -dimers with a separation between rings of about 3.4 \AA (radical), and σ -dimers with a long C–C single bond [1.599(4) \AA] between the symmetry-related C14 atoms (Figures 2–4).

The orange crystals of 6^+ , BPh_4^- were found to belong to the triclinic space group $P\bar{1}$. There were one cation, $[\text{C}_{70}\text{H}_{74}\text{BN}_2\text{O}_2]^+$, one anion, $[\text{BC}_24\text{H}_{20}]^-$, and two acetonitrile solvent molecules present in the asymmetric unit. Enantiomers of the cation exist as weak π -dimers with a separation between the molecular planes of about 3.56 \AA (Figure 2).

The black crystals of **6a** gave a monoclinic unit cell (space group $P2(1)/c$, $Z = 4$), and the molecule exists as a π -dimer with a separation between the molecular planes of about 3.4 \AA (Figures 3 and 5); on the basis of the magnetic data, we refer to **6a** as the paramagnetic π -dimer.

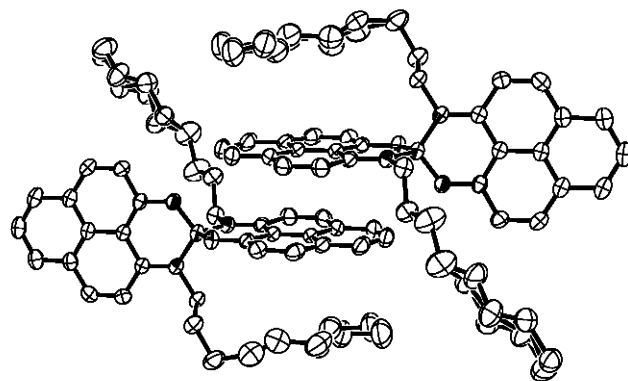


Figure 2. X-ray structure of 6^+ , BPh_4^- . Enantiomers of the cation exist as weak π -dimers with a separation between the molecular planes of about 3.56 \AA . The anion BPh_4^- and two acetonitrile molecules are not shown.

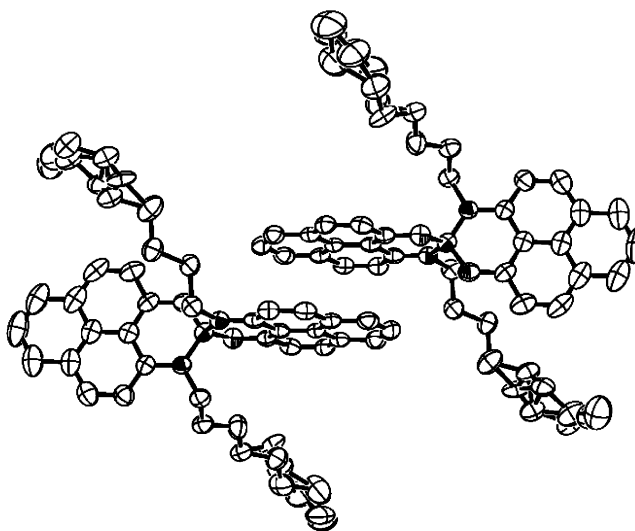


Figure 3. X-ray structure of spirobiphenalenyl neutral radical **6a**. The molecules exist as paramagnetic π -dimers in which the active carbon atoms superpose, and the distance between the planes of the π -dimer is about 3.4 \AA .

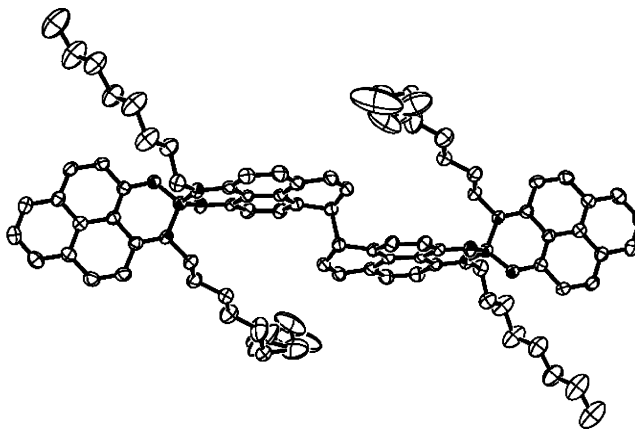


Figure 4. X-ray structure of σ -dimer **6b**. The molecule is located at an inversion center, and the C–C single bond between C14 and its symmetry-related atom is 1.599(4) \AA . Both of the octyl side chains in **6a** and one of the two side chains in **6b** are disordered.

The black crystals of **6b** gave a triclinic unit cell (space group $P\bar{1}$, $Z = 1$). The C–C single bond between the symmetry-related C14 atoms is significantly longer (1.599(4) \AA) than the normal sp^3 C–C single bond length (1.54 \AA) (Figures 4 and 6). While this bond is relatively unstrained, its length is comparable to

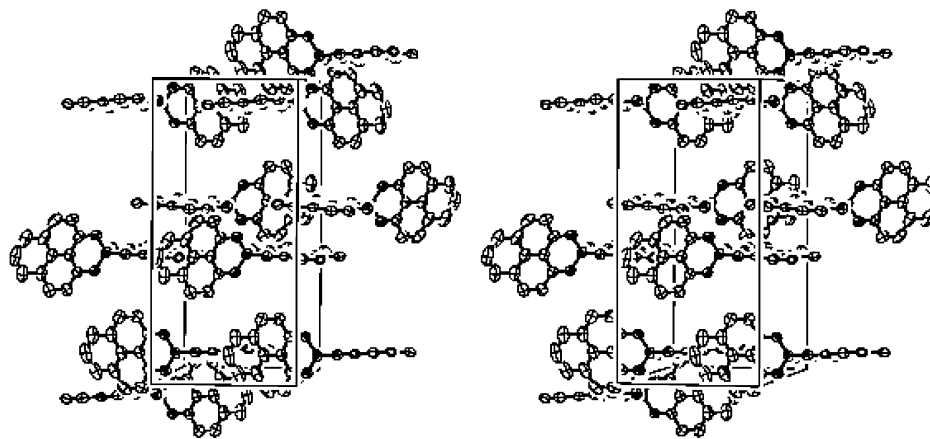


Figure 5. Stereoview of the X-ray structure of **6a** viewed down the x -axis.

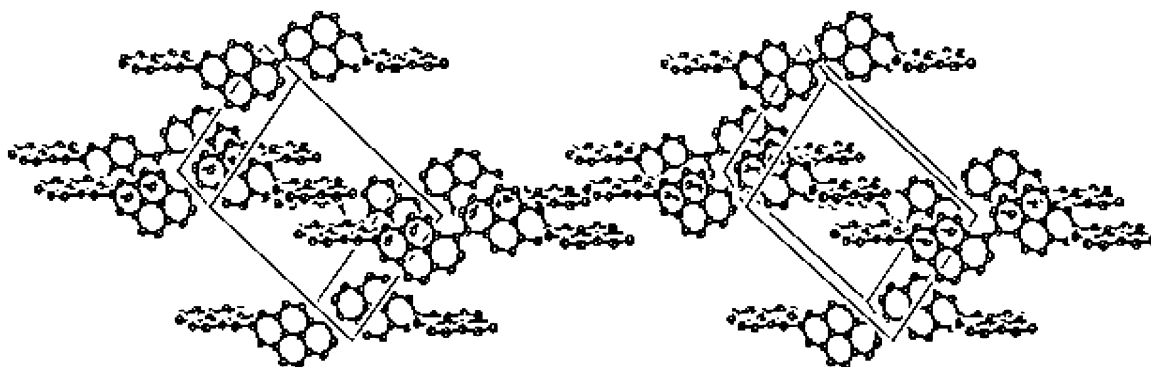


Figure 6. Stereoview of the X-ray structure of **6b** viewed down the x -axis.

those of other strained C–C bonds and to those of carbon σ -bonds that form at the expense of a delocalized π -system. The length of the central C–C bond in Gomberg-type dimers such as hexaphenylethane and its derivatives is generally greater than 1.6 Å,^{5,17,18} although shorter than the bond lengths that occur in charged π -dimers.^{19–26}

The length of the σ -bond in **6b** is comparable to that of the intercege C–C bond (1.597(7) Å) of the (C60[−])₂ dimer. The reversible formation of this dimer occurs at around 220 K.^{27,28} This raises the question as to whether the polymorphs might be interconvertible. However, magnetic susceptibility measurements of **6b** show a diamagnetic state from 5 to 441 K, at which point the material decomposes (Figure 7).

Magnetic Susceptibility of the Polymorphs 6a and 6b. We measured the magnetic susceptibility (χ) of the octyl radical **6a** and the σ -dimer **6b** as a function of temperature (T) in a Faraday balance.⁹

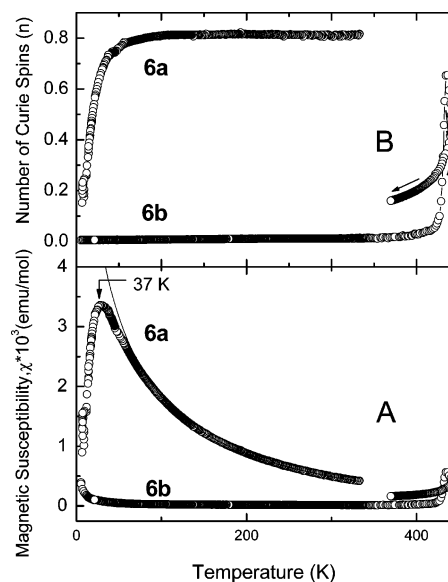


Figure 7. Magnetic susceptibilities of **6a** and **6b** as a function of temperature (A) and the fraction of Curie spins per molecule (B). The solid line is a Curie fit to the data between 100 and 330 K.

Above $T = 37$ K, **6a** shows typical Curie–Weiss behavior with χ of the form $\chi = \chi_0 + C/(T + \Theta)$ ($\chi_0 = -406.48 \times 10^{-6}$ emu/mol, $C = 0.30$ emu·K/mol, $\Theta = 37$ K). In Figure 7B, we use the function $n = 8(\chi - \chi_0)(\Theta + T)/3$ to obtain the number of Curie spins per molecule (n) as a function of temperature (T). The plot shows that, in the solid state, **6a** behaves as a free radical with close to one spin per molecule. The only proviso to this statement occurs at low temperatures, where the spins

- (16) Huang, J.; Kertesz, M. *J. Am. Chem. Soc.* **2003**, *125*, 13334–13335.
- (17) McBride, J. M. *Tetrahedron* **1974**, *30*, 2009–2022.
- (18) Kaupp, G.; Boy, J. *Angew. Chem., Int. Ed. Engl.* **1997**, *36*, 48–49.
- (19) Del Sesto, R. E.; Miller, J. S.; Lafuente, P.; Novoa, J. J. *Chem.–Eur. J.* **2002**, *8*, 4894–4808.
- (20) Gabriel, J.-C. P. *Mater. Res. Soc. Symp. Proc.* **2003**, *762*, Q.12.17.11.
- (21) Ganesan, V.; Rosokha, S. V.; Kochi, J. K. *J. Am. Chem. Soc.* **2003**, *125*, 2559–2571.
- (22) Lu, J.; Rosokha, S. V.; Kochi, J. K. *J. Am. Chem. Soc.* **2003**, *125*, 12161–12171.
- (23) Jung, Y.; Head-Gordon, Y. *Phys. Chem. Chem. Phys.* **2004**, *6*, 2008–2011.
- (24) Miller, J. S.; Zhang, J. H.; Reiff, W. M.; Dixon, D. A.; Preston, L. D.; Reis, A. H.; Gebert, E.; Extime, M.; Troup, J.; Epstein, A. J.; Ward, M. D. *J. Phys. Chem.* **1987**, *91*, 4344–4360.
- (25) Novoa, J. J.; Lafuente, P.; Del Sesto, R. E.; Miller, J. S. *Angew. Chem., Int. Ed.* **2001**, *40*, 2540–2543.
- (26) Vazquez, C.; Calabrese, J. C.; Dixon, D. A.; Miller, J. S. *J. Org. Chem.* **1993**, *58*, 65–81.
- (27) Reed, C. A.; Bolskar, R. D. *Chem. Rev.* **2000**, *100*, 1075–1120.

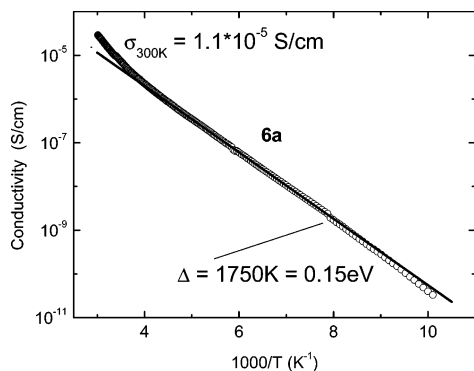


Figure 8. Single-crystal conductivity of **6a** as a function of temperature, measured along the needle axis.

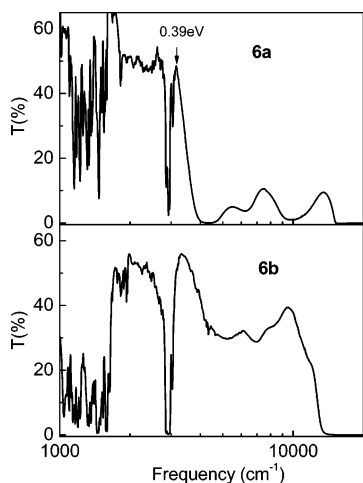


Figure 9. Single-crystal IR and UV-vis transmission spectra of **6a** and **6b**. The average sizes of the single crystals are the following: length 10–11 mm, width 300–400 μm , thickness 5–7 μm (**6a**) and length 4–5 mm, width 200 μm , thickness 46 μm (**6b**).

couple antiferromagnetically below 37 K. However, **6b** shows diamagnetic behavior in the temperature range $T = 5\text{--}441$ K, thereby demonstrating the absence of unpaired electrons in the octyl σ -dimer **6b** (Figure 7).

Electrical Resistivity 6a and 6b. The electrical resistivity (ρ) of about five crystals of **6a** was measured using four-probe inline contacts along the long axis of the blades.⁹ A number of crystals were evaluated over the full temperature range from 100 to 330 K with identical results.

The conductivity of **6a** increases with temperature to give a room-temperature conductivity of $\sigma = 1.1 \times 10^{-5}$ S/cm. It is possible to fit the low-temperature data (Figure 8) to an exponential, extract an activation energy, $E_a = 0.15$ eV, and infer an energy gap, $E_g(\text{transport}) = 2\Delta = 0.3$ eV. The resistivity of the octyl σ -dimer **6b** exceeded the measurement capability of our experiment, and we conclude that the conductivity of this crystalline form is extremely low.

Electronic Excitations in Solid-State 6a and 6b. Single-crystal transmittance spectroscopy (Figure 9) shows that the octyl radical **6a** is near-IR-opaque while the octyl σ -dimer **6b** is near-IR-transparent in the range 3500–10000 cm^{-1} (Figure 10);¹³ this technique provided the most straightforward distinction between the crystalline forms. The absorptions in the mid-IR between 450 and 3100 cm^{-1} are due to the molecular vibrations. There is a characteristic peak at a frequency of 1632

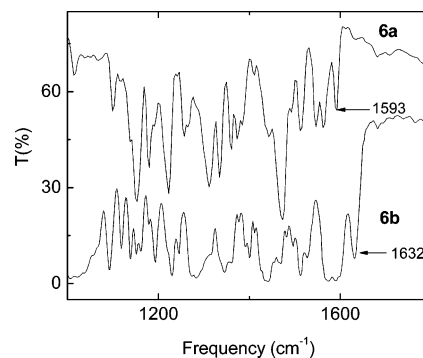


Figure 10. Mid-IR region of single-crystal IR transmission spectra of octyl radical **6a** and octyl σ -dimer **6b**. The peak at a frequency of 1632 cm^{-1} in **6b** is assigned to the C=C stretch, which is absent in **6a**.

cm^{-1} in **6b** due to the C=C stretch, which is absent in **6a**. In the spectrum of the radical **6a**, we find an optical energy gap, $E_g(\text{optical}) = 0.39$ eV (~ 3150 cm^{-1}), together with three absorbance peaks (0.55, 0.78, and 1.19 eV). All of these excitations occur in the near-infrared region, and measurements in the visible confirm that the material is semi-transparent in the region 1–2 eV, accounting for the red color of very thin crystals in transmission. In analogy with crystalline **5** ($R = C_6H_{13}$) we propose that the octyl radical **6a** corresponds to a degenerate Mott–Hubbard insulator with a localized ground state.^{9–12,29,30} This model naturally accommodates the Curie-type magnetic susceptibility behavior with one independent spin per molecule that is observed in these compounds.^{9,10}

Conclusion and Summary

The dimerization observed for **6a** ($R = C_8H_{17}$) prompted us to review the crystallization of the other neutral spirophenalenyl radicals, but as far as we can tell the behavior of **6a** is unique; even when we employed the same conditions for crystal growth that led to **6b**, other members of this series^{9,10} did not produce σ -dimers. Thus, we have presented the preparation, crystallization, and characterization of a C–C σ -bond driven radical dimer with an occurrence domain of unprecedented subtlety. The solid forms crystallize as nonsolvates from the same solvent to give rise to an insulator and a semiconductor.

Experimental Section

Materials. Boron trichloride (Aldrich), sodium tetraphenylborate (Aldrich), and cobaltocene (Strem) were all commercial products and were used as received. 9-Hydroxy-1-oxophenalene was synthesized according to literature procedures.^{31,32} Toluene was distilled from sodium benzophenone ketyl just prior to use. Acetonitrile was distilled from P_2O_5 and then redistilled from CaH_2 immediately before use.

9-N-Octylamino-1-oxophenalene. A mixture of 9-hydroxy-1-oxophenalene (1.96 g, 0.01 mol) and octylamine (20 mL) was refluxed for 20 h under argon. The excess amine was removed on a rotary evaporator to give a yellow solid. The crude product was purified by column chromatography on Al_2O_3 with $CHCl_3$ to give a yellow solid (2.62 g, 85%): yellow plates from heptane; mp 57–57.5 $^\circ\text{C}$; ^1H NMR (CD_3CN) δ 12.25 (br, 1H), 8.08 (d, 1H), 7.8–7.98 (m, 3H), 7.45 (t, 1H), 7.33 (d, 1H), 6.87 (d, 1H), 3.56 (dt, 2H), 1.72–1.82 (m, 2H),

(28) Konarev, D. V.; Khasanov, S. S.; Otsuka, A.; Saito, G. *J. Am. Chem. Soc.* **2002**, *124*, 8520–8521.

(29) Chi, X.; Itkis, M. E.; Reed, R. W.; Oakley, R. T.; Cordes, A. W.; Haddon, R. C. *J. Phys. Chem. B* **2002**, *106*, 8278–8287.

(30) Chi, X.; Tham, F. S.; Cordes, A. W.; Itkis, M. E.; Haddon, R. C. *Synth. Met.* **2003**, *133–134*, 367–372.

1.25–1.55 (br, 10H), 0.88 (t, 3H). Anal. Calcd for $C_{21}H_{25}ON$: C, 82.04; H, 8.20; N, 4.56. Found: C, 82.06; H, 8.23; N, 4.74.

Preparation of $6^+, Cl^-$. 9-*N*-Octylamino-1-oxophenale (1.54 g, 5 mmol) in toluene (60 mL) was treated with boron trichloride in dichloromethane (2.5 mL, 2.5 mmol) under argon in the dark, and the mixture was refluxed overnight. The yellow solid was isolated by filtration (1.4 g, 90%): IR (ATR, 4000–680 cm^{-1}) 3001 (vw), 2924 (m), 2848 (w), 1626 (m), 1585 (m), 1569 (s), 1514 (s), 1488 (vw), 1468 (w), 1446 (w), 1392 (m), 1358 (m), 1294 (vs), 1247 (m), 1225 (vw), 1198 (m), 1171 (w), 1133 (m), 1101 (w), 1079 (m), 1022 (vs), 960 (w), 930 (m), 898 (s), 886 (w), 867 (vs), 836 (m), 824 (m), 766 (m), 711 (w).

Preparation of $6^+, BPh_4^-$. A solution of 0.5 g of $NaBPh_4$ in 20 mL of MeOH was added to a solution of $1^+, Cl^-$ (0.6 g) in 40 mL of MeOH. A yellow precipitate formed immediately. The mixture was stirred for 5 min, and 0.58 g (68%) of yellow solid was separated and stored in the dark. The yellow product was purified by recrystallization from acetonitrile: 1H NMR (CD_3CN) δ 8.56 (d, 2H), 8.45 (d, 2H), 8.35 (m, 4H), 7.84 (t, 2H), 7.46 (m, 4H), 7.27 (br, 8H), 6.99 (t, 8H), 6.84 (t, 4H), 3.66 (br, 2H), 3.29 (br, 2H), 1.74 (br, 4H), 1.10 (vbr, 20H), 0.59 (t, 6H); IR (ATR, 4000–680 cm^{-1}) 3054 (w), 2926 (m), 2853 (w), 1627 (s), 1595 (m), 1584 (m), 1573 (s), 1515 (s), 1471 (m), 1446 (m), 1425 (w), 1413 (w), 1389 (m), 1357 (m), 1333 (w), 1294 (s), 1244 (m), 1192 (m), 1167 (m), 1136 (m), 1101 (w), 1023 (m), 900 (m), 845 (s), 824 (w), 766 (w), 745 (w), 731 (m), 704 (s).

Crystallization of $6a$. All operations were performed in the dark in an argon atmosphere drybox. Solid Cp_2Co (10 mg) was added carefully to a solution of $6^+, BPh_4^-$ (30 mg) in 10 mL of degassed acetonitrile (three freeze–pump–thaw cycles). The solution was allowed to stand overnight in the dark, which resulted in black blades of radical $6a$ (12 mg, 60%). Anal. Calcd for $C_{42}H_{48}O_2N_2B$: C, 80.89; H, 7.76; N, 4.49; B, 1.73. Found: C, 80.41; H, 7.71; N, 4.63; B, 1.71.

Crystallization of $6b$. Solid Cp_2Co (12 mg) was added carefully to a solution of $6^+, BPh_4^-$ (30 mg) in 10 mL of degassed acetonitrile (three freeze–pump–thaw cycles). The solution was prepared under visible light in an argon atmosphere drybox and allowed to stand overnight, which resulted in black needles of the σ -dimer $6b$ (13 mg, 66%). Anal. Calcd for $C_{84}H_{96}O_4N_4B_2$: C, 80.89; H, 7.76; N, 4.49; B, 1.73. Found: C, 80.96; H, 7.79; N, 4.68; B, 1.68.

X-ray Crystallography. Data were collected on a Bruker SMART 1000 platform CCD X-ray diffractometer (Mo radiation, $\lambda = 0.71073$ Å, 50 kV/40 mA power). An orange crystal of $6^+, BPh_4^-$ gave a triclinic unit cell (space group $P\bar{1}$, $Z = 2$), with unit cell parameters $a = 14.475(3)$ Å, $b = 14.650(3)$ Å, $c = 16.026(3)$ Å, $\alpha = 73.246(4)^\circ$, $\beta = 67.638(4)^\circ$, $\gamma = 69.852(4)^\circ$, and $V = 2898.2(9)$ Å³. The structure was refined with 9750 reflections, yielding $R = 0.0531$. There were one cation, $[C_{42}H_{48}BN_2O_2]^+$, one anion, $[B(C_6H_5)_4]^-$, and two acetonitrile solvent molecules present in the asymmetric unit. The octyl side chains attached to N9 and N19 were disordered. The disordered site occupancy ratios were 80%/20% and 67%/33%, respectively.

A black crystal of $6a$ gave a monoclinic unit cell (space group $P2(1)/c$, $Z = 4$), with unit cell parameters $a = 17.323(3)$ Å, $b = 20.281(5)$ Å, $c = 9.7394(17)$ Å, $\alpha = 90^\circ$, $\beta = 93.740(6)^\circ$, $\gamma = 90^\circ$, and $V = 3414.4(12)$ Å³. The structure was refined with 4176 reflections,

yielding $R = 0.0671$. Full details, including bond lengths and bond angles, are given in the Supporting Information.

A black crystal of $6b$ gave a triclinic unit cell (space group $P\bar{1}$, $Z = 1$), with unit cell parameters $a = 9.1350(15)$ Å, $b = 12.826(2)$ Å, $c = 15.925(3)$ Å, $\alpha = 103.674(4)^\circ$, $\beta = 98.411(4)^\circ$, $\gamma = 103.936(4)^\circ$, and $V = 1718.2(5)$ Å³. The structure was refined with 5867 reflections, yielding $R = 0.0506$. There was half a molecule of $6b$ present in the asymmetric unit. The molecule was located at the inversion center. One of the two octyl side chains was disordered (site occupancy ratio of 65%/35%).

Magnetic Susceptibility Measurements. The magnetic susceptibility of $6a$ and $6b$ were measured over the temperature range 7–332 K and 5–441 K respectively on a George Associates Faraday balance operating at 0.5 T.

Conductivity Measurements. The single-crystal conductivity, σ , of $6a$ was measured in a four-probe configuration. The in-line contacts were made with silver paint. The sample was placed on a sapphire substrate, and electrical connections between the silver paint contacts and substrate were made by thin, flexible 25 μm diameter silver wires to relieve mechanical stress during thermal cycling of the sample. The temperature dependence of the conductivity was measured in the range 330–100 K. Below 100 K the sample resistance exceeded 10^{13} Ω , the limit of the experiment. The data are presented for a crystal with dimensions $6 \times 200 \times 3000$ μm^3 .

Conductivity was measured in a custom-made helium variable-temperature probe using a Lake Shore 340 temperature controller. A Keithley 236 unit was used as a voltage source and current meter, and two 6517A Keithley electrometers were used to measure the voltage drop between the potential leads in a four-probe configuration.

Single-Crystal IR and UV–Vis Transmission Spectroscopy. The infrared transmission measurements were carried out on a Nicolet Nexus 670 ESP FTIR spectrometer integrated with a Continuum Thermo-Nicolet FTIR microscope.

For the UV–vis spectral range, a sapphire substrate was coated with a 2500 Å thick silver film so as to produce a long narrow slit (60×2000 μm^2). Thin single crystals of $6a$ and $6b$ with dimensions $6 \times 300 \times 2500$ μm^3 and $46 \times 200 \times 2500$ μm^3 were placed on the substrate so that the open slit was completely covered by the crystal. In the finished mounting, only radiation transmitted through the sample was detected (no stray light). Data were normalized on the spectra of the slit itself without the sample.

Acknowledgment. This work was Supported by the Office of Basic Energy Sciences, Department of Energy, under Grant No. DE-FG03-01ER45879.

Supporting Information Available: Tables of crystallographic and structural refinement data, atomic coordinates, bond lengths and angles, and anisotropic thermal parameters (PDF, CIF). This material is available free of charge via the Internet at <http://pubs.acs.org>.

JA046243Z

(31) Koelsch, C. F.; Anthes, J. A. *J. Org. Chem.* **1941**, *6*, 558–565.

(32) Haddon, R. C.; Rayford, R.; Hirani, A. M. *J. Org. Chem.* **1981**, *46*, 4587.